ELSEVIER

Analytica Chimica Acta 391 (1999) 73–82

ANALYTICA CHIMICA ACTA

Hydrogen peroxide sensor based on horseradish peroxidase-labeled Au colloids immobilized on gold electrode surface by cysteamine monolayer

Yi Xiao, Huang-Xian Ju, Hong-Yuan Chen*

Department of Chemistry, The State Key Laboratory of Coordination Chemistry, Nanjing University, 210093, Nanjing, China

Received 15 October 1998; received in revised form 10 February 1999; accepted 13 February 1999

Abstract

A novel strategy to construct a sensitive amperometric sensor of H_2O_2 was described. Horseradish peroxidase (HRP) was successfully immobilized on nanometer-sized Au colloids, which were supported by thiol-tailed groups of cysteamine monolayer. The thiol-tailed groups were formed through the covalent binding of glutaraldehyde on a cysteamine-modified gold electrode. With the aid of the catechol mediator in the solution, HRP-labeled Au colloids displayed excellent electrocatalytical response to the reduction of H_2O_2, which increased with decreasing size of Au colloids. The sensors responded to H_2O_2 in the concentration range of 0.39 μM–0.33 mM, and reached 95% of the steady-state current in less than 5 s with the detection limit of 0.15 μM. The response showed a Michaelis–Menten behavior at larger H_2O_2 concentrations. The K_M^{app} values for the sensors based on different sized HRP-labeled Au colloids (colloid A–D) were found to be 0.11, 0.094, 0.054 and 0.064 mM, respectively. The low K_M^{app} values demonstrated that HRP immobilized on Au colloids exhibited a high affinity to H_2O_2 with no loss of enzymatic activity.

Keywords: Self-assembled monolayers; HRP-labeled Au colloids; Cysteamine; Hydrogen peroxide; Sensors; Electrochemical sensors

1. Introduction

The determination of hydrogen peroxide is of great importance. It is not only a by-product of several highly selective oxidases but also an essential mediator in food, pharmaceutical, clinical, industrial and environmental analyses [1–3]. Many techniques have been employed for the determination of hydrogen peroxide, for example, titrimetry [4], spectrometry [5], chemiluminescence [6] and electrochemistry [7–25]. The first three techniques have obvious drawbacks because they are time-consuming, subject to interferences, and need expensive reagents. Electrochemical methods overcome these drawbacks. Many electrochemical techniques make use of the reduction of H_2O_2 by the catalysis of immobilized horseradish peroxidase (HRP) to construct mediated-free HRP-based sensors [7–12] or mediated HRP-based sensors [13–25]. These mediated HRP-based sensors could hold the detection limits as low as 10^{-7}–10^{-8} M by use of electron transfer mediators such as $[Ru(NH_3)_5py]^{2+}$ [16], ferrocene derivatives [16,17], tetrathiafulvalene [18], or phenazine methosulfate

*Corresponding author. Tel.: +86-25-335-3198; fax: +86-25-331-7761; e-mail: hychen@netra.nju.edu.cn

0003-2670/99/$ – see front matter
PII: S0003-2670(99)00196-8

[19]. However, the application and development of biosensors have been limited due to the lack of a simple and stable enzyme immobilization approach and the denaturation of immobilized enzymes.

The assembly of enzyme monolayers on Au surfaces has been reported by Willner and coworkers [26–28]. The metal colloidal film has also been used as a basic interface to construct a redox-active monolayer [29–32]. Generally, direct adsorption of proteins onto naked metal surfaces can frequently result in their denaturation and the loss of bioactivity. However, the adsorption of such proteins on the surface of metal nanoparticles may retain their bioactivity [33,34]. Thus, colloidal gold provides an environment similar to the native environment of redox proteins. The biosensors based on the enzyme-covered nanoparticles electrodeposited on a platinum gauze or a glassy carbon surface have been reported [33,35]. Crumbliss and co-workers [35] deposited HRP-gold sol on the surface of a flat glassy carbon electrode to obtain a mediator-free H_2O_2 sensor, and presented a possible mechanism for the direct electron transfer between the redox center of HRP and the surface of a HRP-gold sol modified electrode.

In this work, a monolayer containing the thiol-tailed groups of cysteamine was prepared through covalent binding of glutaraldehyde on cysteamine-modified gold electrode surface. The Au colloids adsorbed covalently on the thiol monolayer providing an active matrix for the immobilization of HRP, which greatly amplified the surface coverage of the functional monolayer. With the aid of the electron mediator-catechol, the smaller sized HRP-labeled Au colloids exhibited a higher amperometric response to the reduction of H_2O_2 than that observed on the larger sized HRP-labeled Au colloids. Experimental results indicated that HRP immobilized on Au colloids displayed a high affinity to H_2O_2, excellent sensitivity and stability with long-term maintenance of bioactivity.

2. Experimental

2.1. Reagents and apparatus

Horseradish peroxidase (HRP, E.C.1.11.1.7, RZ>3.0, *A*>250 U/mg) and cysteamine were purchased from Sigma. The 25% glutaraldehyde was obtained from Shanghai Biochemical Reagent (China). The concentrations of more diluted hydrogen peroxide solutions were determined by titration with cerium (IV) to a ferroin end-point [4]. 0.1 M phosphate buffer solutions (PB) were prepared with K_2HPO_4 and KH_2PO_4. $AuCl_3HCl{\cdot}4H_2O$ (Au%> 48%) and all other chemicals were of analytical grade and used without further purification. All solutions were made up with twice-distilled water.

Electrochemical measurements were performed with a three-electrode system comprising a platinum wire as auxiliary electrode, a saturated calomel electrode (SCE) as reference, against which all potentials were measured, and the H_2O_2 sensor as working electrode. The electrodes were connected to a BAS-100B electrochemical analyzer with a PA-1 preamplifier (Bioanalytical System, USA). Cyclic voltammetric measurements were done in thermostated and unstirred electrochemical cell at 37±0.2°C in a Faraday cage. Amperometric experiments were carried out in a thermostated and stirred cell at 37±0.2°C by applying a potential step of −100 mV to the working electrode. Aliquots of H_2O_2 standard solution were successively added to the solution. Current–time data were recorded after a steady-state current had been achieved. All experimental solutions were deaerated by highly pure nitrogen for 10 min, and a nitrogen atmosphere was kept over the solutions during measurements.

2.2. Preparation of Au colloids

All glasswares used in the following procedures were cleaned in a bath of freshly prepared 3:1 HNO_3–HCl, rinsed thoroughly in twice-distilled water and dried in air. $HAuCl_4$ and Na_3 citrate solutions need to be filtered through a 22 μm microporous membrane filter prior to use. Preparations were stored in dark glass bottles at 4°C. Au colloids were prepared according to the literature [36] by adding Na_3 citrate solution to a boiling $HAuCl_4$ aqueous solution. The molar ratios of $HAuCl_4$/Na_3 citrate used for the preparation of different nanometer-sized colloids were as follows: colloid A, 0.30; colloid B, 0.75; colloid C, 1.00; colloid D, 1.51. The diameters of Au colloid A–D were 16±2.3 nm, 24±2.1 nm, 42±2.6 nm and 51±5.3 nm, respectively, which were measured by using transmission electron microscopy (TEM).

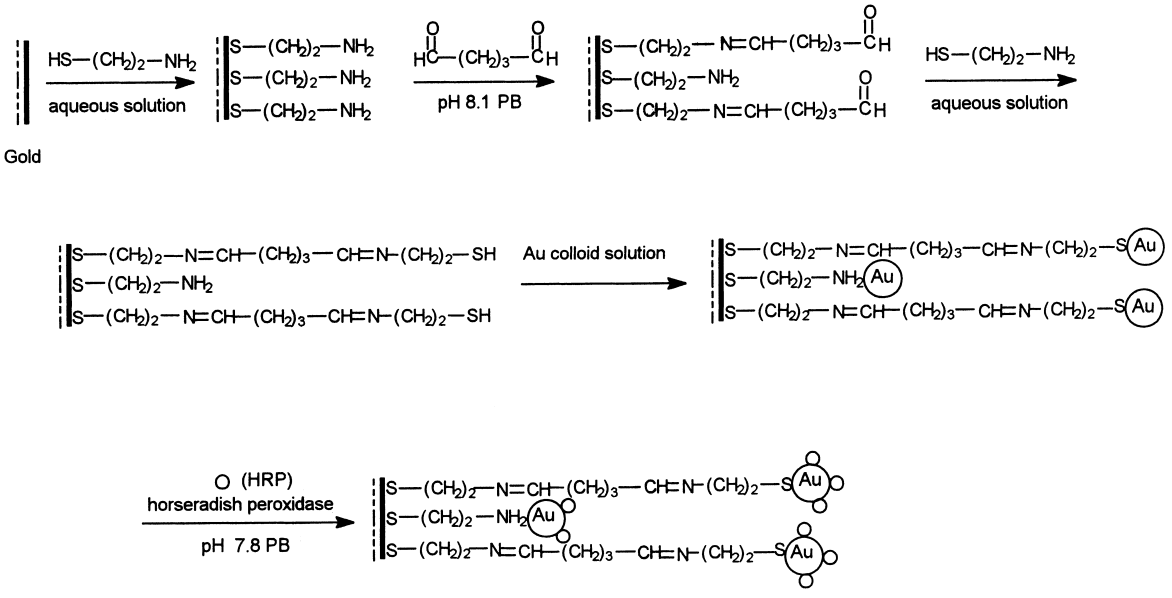

Scheme 1. Preparation process of H_2O_2 sensor.

2.3. Construction of H_2O_2 sensor

Gold electrodes were prepared by sealing polycrystalline gold wires (>99.99%) in soft glass tubes. The gold electrodes were abraded with successively finer grades of SiC paper and polished to a mirror-like surface with 0.3 and 0.05 μm alumina slurry on microcloth pads (Buehler), followed by rinsing with water and ethanol and briefly cleaning in an ultrasonic bath. The geometric area of $(1.31\pm0.16)\times10^{-3}$ cm^2 was obtained by using cyclic voltammetry in 0.1 M KNO_3 solution containing 1.01 mM $K_3[Fe(CN)_6]$. A roughness factor of 1.4±0.2 was calculated from the ratio of the real to the geometric area. The real area was calculated by the integration of cathodic peak during the redox of superficial gold in 1.0 M H_2SO_4 [37].

The cysteamine monolayer was firstly prepared by soaking a clean gold electrode in 18 mM cysteamine aqueous solution for 4 h at room temperature in darkness. After the electrode was thoroughly rinsed with water to remove physically adsorbed cysteamine, it was immersed in pH 8.1 PB containing 12% (v/v) glutaraldehyde solution for 12 h, and was rinsed with water. Then, the electrode was placed into 18 mM cysteamine solution for 12 h to form the Schiff base between the aldehyde group of glutaraldehyde and the amino-group of cysteamine, and followed by dipping it in an Au colloid solution (colloid A, B, C, or D) for 10 h at 4°C. Finally, the covalent attachment of HRP to Au colloid was performed by incubating the electrode in 5 mg/ml HRP PB (pH 7.8) for 12 h to fabricate the H_2O_2 sensor. After thoroughly rinsing the sensor with pH 7.0 PB, it was kept in the same PB at 4°C. The preparation process of H_2O_2 sensor is shown in Scheme 1. The association of the HRP to the colloid surface is possibly due to the interaction between cysteine or NH_3^+-lysine residues of HRP and the Au colloid surface.

3. Results and discussion

3.1. Electrochemical characteristics of catechol on HRP-labeled Au colloids associated with cysteamine self-assembled monolayer (SAM)

The cyclic voltammograms of 0.81 mM catechol in pH 6.9 PB at gold electrodes modified with different sized HRP-labeled Au colloids showed a couple of redox peaks (Fig. 1 for colloid A and D). With increasing size of Au colloids, the peak currents

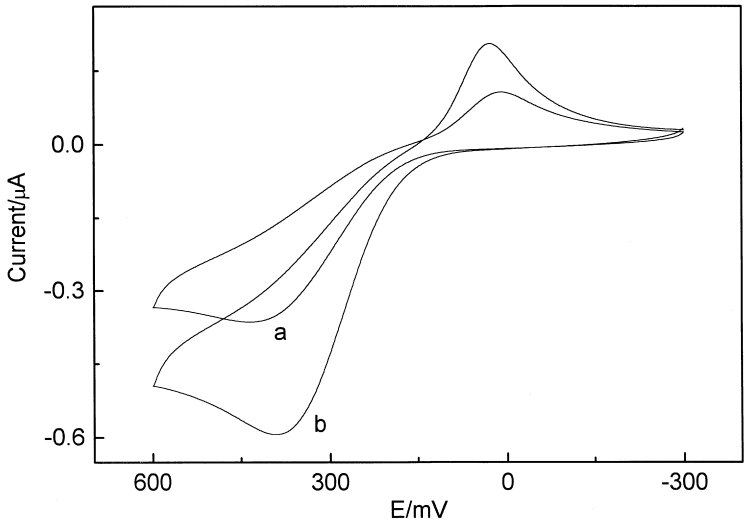

Fig. 1. Cyclic voltammograms of 0.81 mM catechol in pH 6.9 PB at (a) HRP-labeled colloid A modified electrode; (b) HRP-labeled colloid D modified electrode at 50 mV/s.

gradually increased and the difference between peak potentials (ΔE_p) decreased. Thus, the Au colloids with larger size (colloid C and D) are favorable to the redox reaction of catechol, producing a higher amperometric response. The phenomenon can be ascribed to the greater retardation to the redox processes of catechol resulting from the dense gold film [31]. At all of four Au colloids (Fig. 2 for colloid A, as instance), there were linear relations between the redox peak currents and the square root of scan rate ($v^{1/2}$) in the presence of 19 μM H_2O_2. In the meantime, ΔE_p increased with increasing scan rate. Thus, the oxidized and reduced forms of catechol in the solution did not adsorb on modified electrode surface.

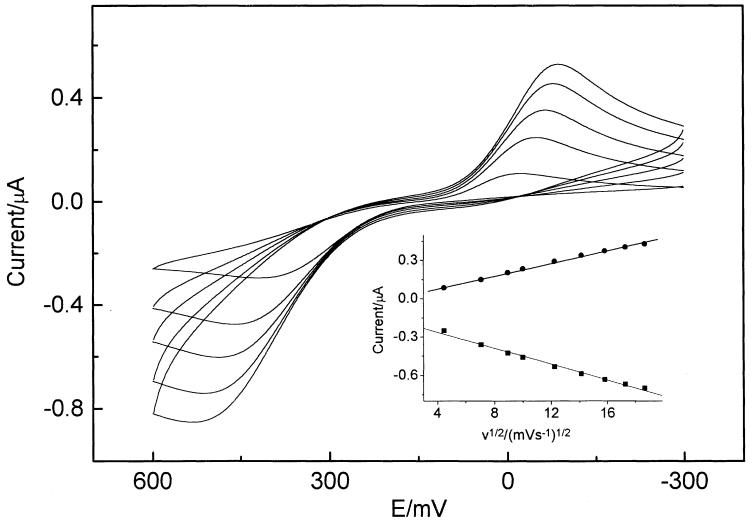

Fig. 2. Cyclic voltammograms of 0.81 mM catechol in pH 6.9 PB at HRP-labeled colloid A modified electrode at 20, 80, 150, 200 and 350 mV/s in the presence of 19 μM H_2O_2. Inset: plots of peak currents versus $v^{1/2}$.

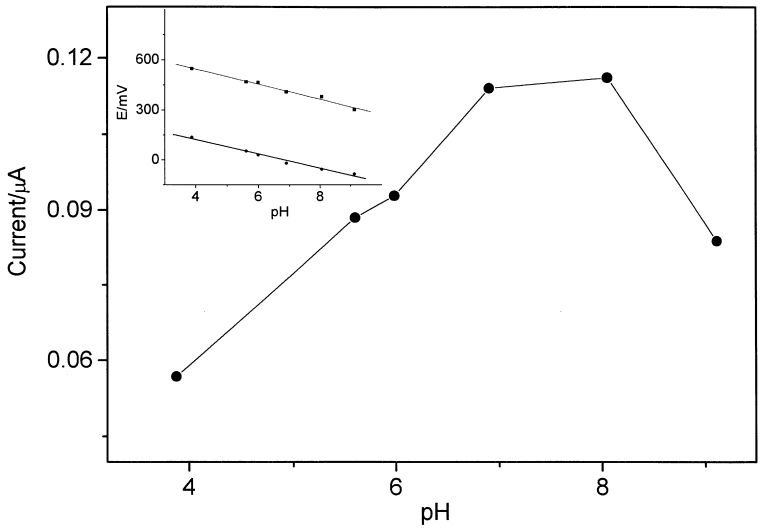

Fig. 3. Effect of pH on the amperometric response of H_2O_2 at HRP-labeled colloid A modified electrode in PB with various pHs containing 0.81 mM catechol and 19 μM H_2O_2. Inset: plots of peak potentials versus pH.

The effect of pH on the reduction current of catechol exhibited a maximum response in the pH range of 7.0–8.0 on HRP-labeled Au colloids with different size in the presence of 19 μM H_2O_2. For example, Fig. 3 shows the dependence of cathodic current on pH at the colloid A-based H_2O_2 sensor. The same result was also observed for soluble peroxidase [14], indicating that the Au colloid matrix did not alter the optimal pH value for the catalytic behavior of peroxidase. Plots of cathodic and anodic peak potentials versus pH gave two lines with the slopes of −42 and −45 mV pH^{-1} in the pH range of 3.9–9.1, respectively. Considering a two-electron transfer process of catechol, the number of H^+ participating in the electrode process was 2.

When changing the catechol concentration from 0.05 to 0.71 mM, the cathodic currents of these H_2O_2 sensors sharply increased in the presence of 19 μM H_2O_2. However, further increase of the catechol concentration did not change the response currents. Such a behavior is typical of a mediator-based sensor [38,39]. At low mediator concentration, the current response was limited by enzyme-mediator kinetics. The high mediator concentration resulted in the response limited by enzyme-substrate kinetics. However, a higher concentration of catechol produced a larger background current. So 0.81 mM catechol is used in the following sections.

3.2. Amperometric response of H_2O_2 sensors based on HRP-labeled Au colloids

The gold nanoparticle films acted as an improved active interface for the immobilization of the redox enzyme can retain the bioactivity of the enzyme [33]. The excellent electrocatalytic behavior of the HRP-labeled Au colloids modified electrode to the reduction of H_2O_2 could be observed (Fig. 4(c)), compared with the Au colloids modified electrode without the attachment of HRP (Fig. 4(a)) in the presence of 0.81 mM catechol. These results indicated that the surface of Au colloid particles has no functional groups to catalyze the reduction of H_2O_2.

Fig. 4 also shows that HRP adsorbed on Au colloids cannot catalyze the reduction of H_2O_2 without the aid of catechol (Fig. 4(b)), compared with the same H_2O_2 sensor in the presence of 0.81 mM catechol (Fig. 4(c)). Here, glutaraldehyde was used as a bifunctional reagent for covalent contacting two amino-groups of cysteamine, and provided an interface containing the thiol-tailed groups for the association with Au colloids on electrode surface. Thus, a long ''molecular bridge'' between the electrode surface and HRP molecules was constructed. Although colloidal gold nanoparticles could function as electron conducting pathways between the prosthetic groups of HRP and

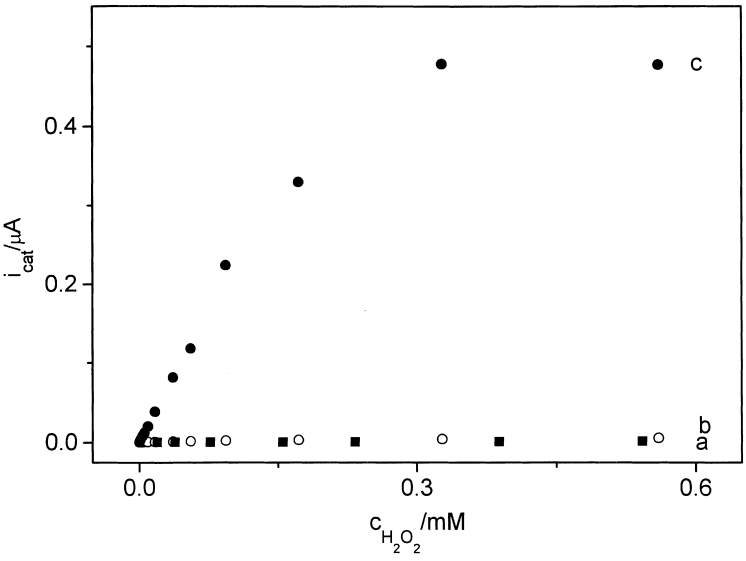

Fig. 4. Amperometric response of (a) colloid A modified electrode without catechol (○), (b) HRP-labeled colloid A modified electrode in the absence of catechol (■) and (c) in the presence of 0.81 mM catechol (●) to successive addition of 19 μM H_2O_2 in pH 6.9 PB at −100 mV.

the electrode surface, the longer space distance made the electron transfer difficult.

When H_2O_2 was added to pH 6.9 PB, the obvious catalytic characteristic appeared with a dramatic increase of the reduction current and a sharp decrease of the oxidation current in the presence of 0.81 mM catechol (Fig. 5, I and II). These phenomena indicated that catechol could effectively shuttle electrons from the gold electrode surface to the redox center of HRP immobilized on Au colloid matrix. The mechanism of

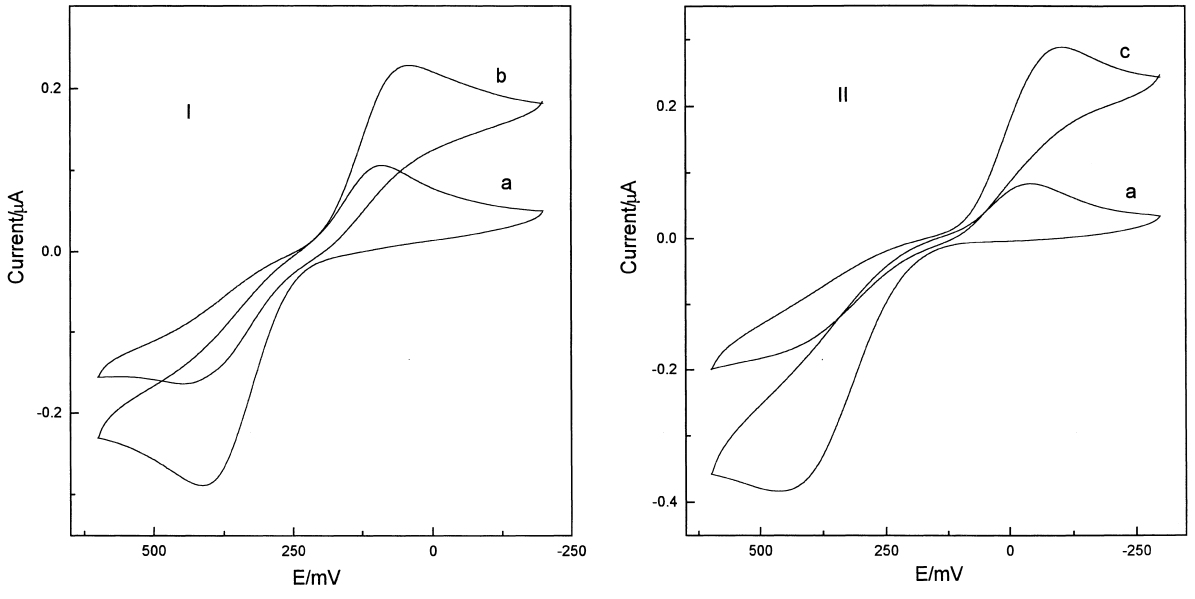

Fig. 5. Cyclic voltammograms of HRP-labeled colloid A modified electrode (I) and HRP-labeled colloid D modified electrode (II) in pH 6.9 PB containing 0.81 mM catechol at 50 mV/s in the absence of H_2O_2 (a) and in the presence of 39 μM H_2O_2 (b) and 66 μM H_2O_2 (c).

H_2O_2 determination can be summarized in the following scheme [40,41]:

$$H_2O_2 + HRP_{(Red)} \rightarrow H_2O + HRP(O)_{(Ox)}$$

$$\uparrow \qquad\qquad \downarrow$$

$$HRP(O)_{(Ox)} + \text{catechol}_{(Red)} \rightarrow HRP_{(Red)} + \text{catechol}_{(Ox)} + H_2O$$

$$\uparrow \qquad\qquad \downarrow$$

and : $\text{catechol}_{(Ox)} + 2e + 2H^+ \rightarrow \text{catechol}_{(Red)}$

Net reaction : $H_2O_2 + 2e + 2H^+ \rightarrow 2H_2O$

With the addition of H_2O_2, the striking decrease of oxidation current of catechol implied that the oxidized form of HRP could be quickly reduced to its native form by catechol. Fig. 5 also shows that the electrocatalytic current on the smaller sized HRP-labeled colloid A is higher than that on the larger sized HRP-labeled colloid D. As well known, the interaction between protein molecules and Au colloid particles is very strong due to the very high surface to volume ratio of Au colloid particles and their high surface energy [35]. Doron and co-workers [31] confirmed that the larger sized Au colloids can discontinuously assemble and the smaller sized Au colloids may generate continuous arrays of particles on the base monolayer. The pack of smaller sized Au colloids bound monolayers are denser than that of the larger sized Au colloids, providing more active binding sites for the immobilization of HRP. Fig. 6 shows the amperometric response of HRP-labeled Au colloid (A–D) modified electrodes to the reduction of H_2O_2 under the steady-state condition. The magnitude of the steady-state current depends on the size of Au colloid particles associated with cysteamine monolayer, which is in agreement with that observed for the redox of bipyridinium units on Au colloid modified siloxane monolayer [31]. The smaller sized HRP-labeled Au colloids (A, B) have higher electrocatalytic activity, compared with the larger sized HRP-labeled Au colloids (C, D).

3.3. Calibration, reproducibility and recovery of H_2O_2 sensors

The steady-state currents gradually increased with the change of applied voltage from +50 to −300 mV (Fig. 7). The increased response could be attributed to the change in driving force for the reduction of oxidized catechol that was produced during the cat-

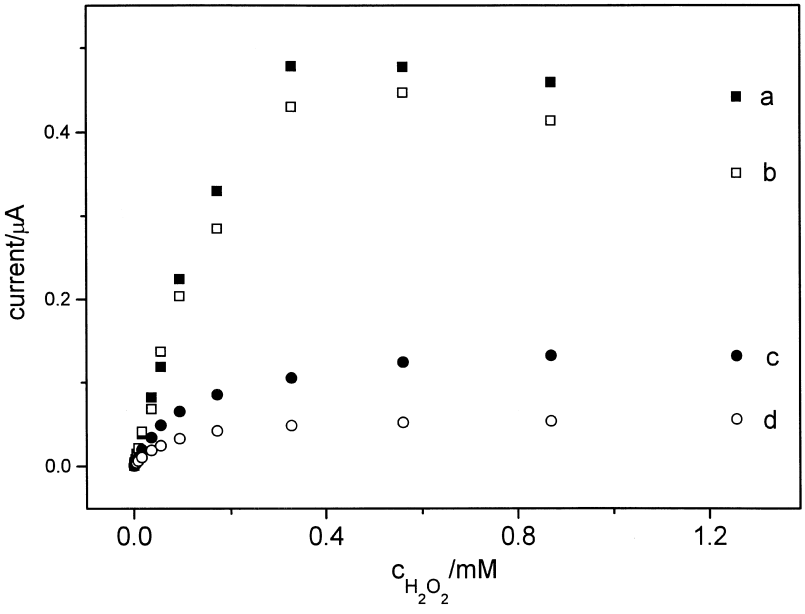

Fig. 6. Amperometric response of HRP-labeled Au colloids with different sizes to the reduction of H_2O_2 ((a): colloid A (■); (b): colloid B (□); (c): colloid C (●); (d): colloid D (○)) in pH 6.9 PB containing 0.81 mM catechol under steady-state condition.

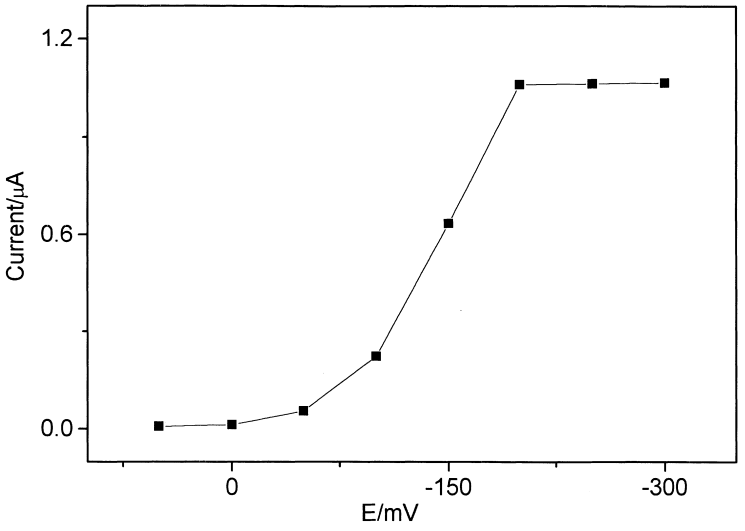

Fig. 7. Dependence of steady-state current on applied voltage at HRP-labeled colloid A modified electrode in pH 6.9 PB containing 0.81 mM catechol in the presence of 0.12 mM H_2O_2.

alytic reaction of enzyme-substrate. Electroreduction of H_2O_2 on HRP-labeled Au colloids was observed at ca. −100 mV. This lower working potential may avoid or decrease the interference caused by some electroactive species (special interference arises from oxygen) in the solution. At the applied voltage of −100 mV, the calibration range of H_2O_2 was 0.39 μM–0.33 mM as shown in Fig. 6 for the smaller

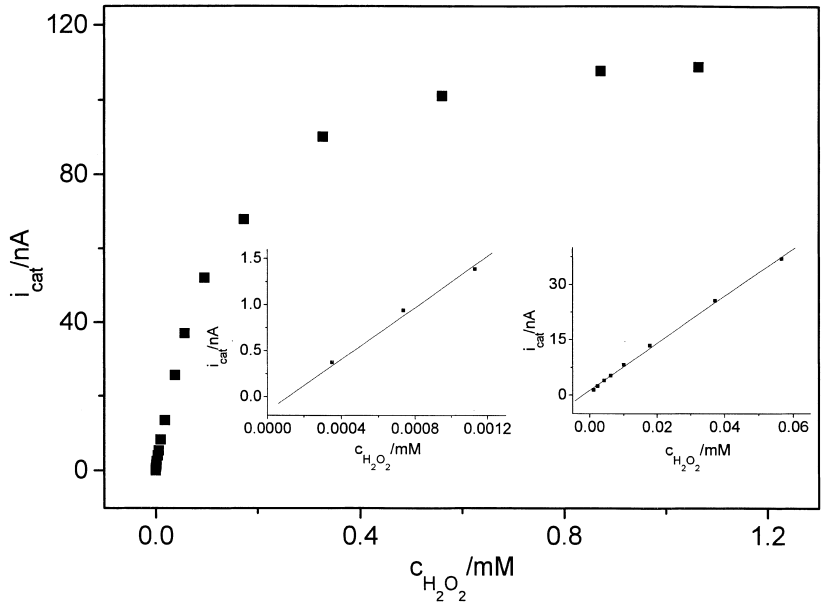

Fig. 8. Amperometric response of HRP-labeled colloid A modified electrode for successive additions of H_2O_2 in pH 6.9 PB containing 0.81 mM catechol. Inset shows linear calibration curves.

Table 1
The recoveries determined at HRP-labeled Au colloids modified electrodes

H_2O_2 (μM)	1.2	3.1	7.0	26
Determined (μM) (Sensor I)	1.1	2.8	6.9	25
Recovery (%) (Sensor I)	92	90	99	96
Determined (μM) (Sensor II)	1.1	3.2	6.8	27
Recovery (%) (Sensor II)	92	103	97	104

Sensor I based on HRP-labeled colloid A; Sensor II based on HRP-labeled colloid D.

sized HRP-labeled Au colloids. The H_2O_2 sensors exhibited a linear calibration range of 0.39–57 μM with a correlation coefficient of 0.996 (n=11) (Fig. 8). Fig. 6 also shows that the amperometric response begins to decrease on the smaller sized HRP-labeled Au colloids, and remains constant on the larger sized HRP-labeled Au colloids when the concentration of H_2O_2 is higher than 0.56 mM. These facts revealed that denaturation of HRP has occurred, and that it was irreversibly transformed into its higher oxidized, inactive form at higher H_2O_2 concentration [42]. The loss of bioactivity of HRP immobilized on the smaller sized Au colloids was easier than that on the larger sized Au colloids at the same H_2O_2 concentration.

These sensors attained 95% of the steady-state currents in less than 5 s during the calibration range of H_2O_2. At a signal-to-noise ratio of 3, the detection limit of H_2O_2 was found to be 0.16 μM. The variation coefficients were 1.5% and 1.6% for over 10 successive assays at the H_2O_2 concentration of 3.1 and 26 μM, respectively. The fabrication reproducibility of four electrodes, made independently, showed an acceptable reproducibility with a variation coefficient of 3.1% for the current determined at 3.1 μM H_2O_2. By a calibration curve method, the recoveries of four H_2O_2 samples in the range 1.2–26 μM are shown in Table 1. The average recovery was 97% with a variation coefficient of 4.7%.

The above H_2O_2 sensors were stored in 0.1 M phosphate buffer (pH 7.0) in refrigerator when not in use. The response of these sensors decreased to 90% after storing for two weeks.

3.4. Determination of the apparent Michaelis–Menten constant

The apparent Michaelis–Menten constant (K_M^{app}), which gives an indication of the enzyme-substrate kinetics, can be obtained from the electrochemical version of the Lineweaver–Burk equation [43]:

$$\frac{1}{I_{SS}} = \frac{I}{I_{max}} + \frac{K_M^{app}}{I_{max}c}$$

where I_{ss} is the steady-state current after the addition of substrate, c is the bulk concentration of the substrate and I_{max} is the maximum current measured under saturated substrate condition. The K_M^{app} was determined by analysis of the slope and intercept for the plot of the reciprocals of the steady-state current versus H_2O_2 concentration. The K_M^{app} values of the H_2O_2 sensors, based on different sized Au colloids (A–D), were found to be 0.11, 0.094, 0.054, 0.064 mM, respectively. These K_M^{app} values were smaller than those reported by Qian et al. [19] and Liu et al. [44] for HRP existing in solution or immobilized on the electrode surface. The smaller K_M^{app} values mean that immobilized HRP possesses higher enzymatic activity, and the present electrodes exhibit higher affinity to H_2O_2 [14]. Although the surface interaction among mediator, colloidal gold and protein is not completely understood yet, HRP immobilized on Au colloids can keep its bioactivity and exhibits a high affinity to H_2O_2. The maintenance of enzymatic activity is in agreement with that reported by Crumbliss and co-workers [33,35]. Moreover, the K_M^{app} values gradually decreases with increasing size of Au colloids, indicating that the retaining of HRP bioactivity and the affinity to H_2O_2 on the larger sized HRP-labeled Au colloids are better than those on the smaller sized HRP-labeled Au colloids. These phenomena may be ascribed to the fact that the larger sized Au colloids could give the HRP molecule more freedom in orientation, and possibly form more conducting channels between the prosthetic groups of HRP and catechol molecules.

Acknowledgements

This project was supported by the National Natural Science Foundation of China (29835110 and 29775010) and Scientific Research Foundation for Returned Overseas Chinese Scholars, Ministry of Education of China.

References

[1] E.S. Forzani, G.A. Rivas, V.M. Solis, J. Electroanal. Chem. 382 (1995) 33.
[2] J. Kulys, L. Gorron, E. Domingues, J. Emneus, H. Jarskog, J. Electroanal. Chem. 372 (1994) 49.
[3] J. Kulys, L. Wang, A. Maksimoviene, Anal. Chim. Acta 274 (1993) 53.
[4] E.C. Hurdis, H. Romeyn Jr., Anal. Chem. 26 (1954) 320.
[5] C. Matsubara, N. Kawamoto, K. Takamura, Analyst 117 (1992) 1781.
[6] K. Nakashima, K. Maki, S. Kawaguchi, S. Akiyama, Y. Tsukamoto, I. Kazuhiro, Anal. Sci. 7 (1991) 709.
[7] A.L. Yaropolov, U. Malouik, S.D. Uarfolomeev, I.V. Berrzin, Dokl. Akad. Nauk SSSR. 249 (1979) 1399.
[8] G. Jonsson, L. Gorton, Electroanalysis 1 (1989) 465.
[9] W.O. Ho, D. Athey, C.J. Mcneil, H.J. Hager, G.P. Evans, W.H. Mullen, J. Electroanal. Chem. 351 (1993) 185.
[10] U. Wollenberger, V. Bogdanovskaya, S. Bobrin, F. Scheller, S.M. Tarasevich, Anal. Lett. 23 (1990) 1795.
[11] A. Morales, F. Cespedes, J. Munoz, E. Martinez-Fabregas, S. Alegret, Anal. Chim. Acta 332 (1996) 131.
[12] U. Wollenberger, J. Wang, M. Ozsoz, E. Gonzalez-Romero, F. Scheller, Bioelectrochem. Bioenerg. 26 (1991) 287.
[13] M.G. Garguilo, N. Huynh, A. Proctor, A.C. Michael, Anal. Chem. 65 (1993) 523.
[14] J. Li, S.N. Tan, H. Ge, Anal. Chim. Acta 335 (1996) 137.
[15] P.D. Sanchez, P.T. Blanco, J.M.F. Alvarez, M.R. Smyth, R. O'Kennedy, Electroanalysis 2 (1990) 303.
[16] J.E. Frew, M.A. Harmer, H.A.O. Hill, S.I. Libor, J. Electroanal. Chem. 201 (1986) 1.
[17] T. Tatsuma, Y. Okawa, T. Watanabe, Anal. Chem. 61 (1989) 2352.
[18] L. Bifulco, C. Cammaroto, J.D. Newman, A.P.F. Turner, Anal. Lett. 27 (1994) 1443.
[19] J. Qian, Y. Liu, H. Liu, T. Yu, J. Deng, J. Electroanal. Chem. 397 (1995) 157.
[20] J. Wang, L-H. Wu, L. Angnes, Anal. Chem. 63 (1991) 2993.
[21] T.J. Ohara, M.S. Vreeke, F. Battaglini, A. Heller, Electroanalysis 5 (1993) 823.
[22] Y. Degani, A. Heller, J. Am. Chem. Soc. 111 (1989) 2357.
[23] J. Ye, R.P. Baldwin, Anal. Chem. 60 (1988) 2263.
[24] J. Janata, M. Josowick, M. Devaney, Anal. Chem. 66 (1994) 201R.
[25] A. Torstensson, L. Gorton, J. Electroanal. Chem. 130 (1981) 199.
[26] I. Willner, E. Katz, B. Willner, Electroanalysis 9 (1997) 965.
[27] M. Lion-Dagan, S. Mark-Tibbon, E. Katz, I. Willner, Angew. Chem., Int. Ed. Engl. 34 (1995) 1604.
[28] I. Willner, N. Lapidot, A. Riklin, R. Kasher, E. Zahavy, E. Katz, J. Am. Chem. Soc. 116 (1994) 1428.
[29] M. Giersig, P. Mulvaney, Langmuir 9 (1993) 3408.
[30] N.D. Denkov, O.D. Velev, P.A. Kralchevsky, I.B. Ivanov, H. Yoshimura, K. Nagayama, Langmuir 8 (1992) 3183.
[31] A. Doron, E. Katz, I. Willner, Langmuir 11 (1995) 1313.
[32] M.J. Hostetler, S.J. Green, J.J. Stokes, R.W. Murray, J. Am. Chem. Soc. 118 (1996) 4212.
[33] A.L. Crumbliss, S.C. Perine, J. Stonehuerner, K.R. Twbergen, J. Zhao, R.W. Henkens, J.P. O'Daly, Biotechnol. Bioeng. 40 (1992) 483.
[34] M. Horisberger, Trends Biochem. Sci. 8 (1983) 395.
[35] J. Zhao, R.W. Henkens, J. Stonehuerner, J.P. O'Daly, A.L. Crumbliss, J. Electroanal. Chem. 327 (1992) 109.
[36] J. Turkevich, P.C. Stevenson, J. Hillier, Disc. Faraday Soc. 11 (1951) 55.
[37] U. Oesch, J. Janata, Electrochim. Acta 28 (1983) 1237.
[38] W. Oungpipat, P.W. Alexander, P. Southwell-Keely, Anal. Chim. Acta 309 (1995) 35.
[39] M. Vreeke, R. Maidan, A. Heller, Anal. Chem. 64 (1992) 3084.
[40] A.C. Maehly, Methods Enzymol. 2 (1995) 801.
[41] H. Durliat, A. Courteix, M. Comtat, Bioelectrochem. Bioenerg. 22 (1989) 197.
[42] S.A. Aderian, A.M. Lambeir, Eur. J. Biochem. 186 (1989) 571.
[43] R.A. Kamin, G.S. Willson, Anal. Chem. 52 (1980) 1198.
[44] D. Silva, R.D. Lindomar, Y. Gushikem, Colloids Surf. B6 (1996) 309.